

Tcf3: a transcriptional regulator of axis induction in the early embryo

Bradley J. Merrill¹, H. Amalia Pasolli¹, Lisa Polak¹, Michael Rendl¹, Maria J. García-García², Kathryn V. Anderson² and Elaine Fuchs^{1,*}

¹Howard Hughes Medical Institute, Laboratory of Mammalian Cell Biology and Development, The Rockefeller University, New York, NY 10021, USA

²Department of Developmental Biology, Sloan Kettering Memorial Institute, New York, NY 10021, USA

*Author for correspondence (e-mail: fuchs1b@rockefeller.edu)

Accepted 15 October 2003

Development 131, 263–274

Published by The Company of Biologists 2004

doi:10.1242/dev.00935

Summary

The roles of Lef/Tcf proteins in determining cell fate characteristics have been described in many contexts during vertebrate embryogenesis, organ and tissue homeostasis, and cancer formation. Although much of the accumulated work on these proteins involves their ability to transactivate target genes when stimulated by β -catenin, Lef/Tcf proteins can repress target genes in the absence of stabilized β -catenin. By ablating Tcf3 function, we have uncovered an important requirement for a repressor function of Lef/Tcf proteins during early mouse development. *Tcf3*^{-/-} embryos proceed through gastrulation to form mesoderm, but they develop expanded and often duplicated axial mesoderm structures, including

nodes and notochords. These duplications are preceded by ectopic expression of *Foxa2*, an axial mesoderm gene involved in node specification, with a concomitant reduction in *Lefty2*, a marker for lateral mesoderm. By contrast, expression of a β -catenin-dependent, Lef/Tcf reporter (TOPGal), is not ectopically activated but is faithfully maintained in the primitive streak. Taken together, these data reveal a unique requirement for Tcf3 repressor function in restricting induction of the anterior-posterior axis.

Key words: Wnt, Gastrulation, Tcf3, Node, Axis

Introduction

Wnt signaling guides cell fate decisions in many physiological contexts, and the molecular nature of its signal transduction provides the Wnt pathway with the ability to have varied effects on cells. Although the stability of β -catenin is central to the activation of Wnt signaling target genes, Lef/Tcf proteins also play pivotal roles, tailoring the transcriptional output to suit particular cellular contexts. An intensive subject of investigation has been to elucidate how Lef/Tcfs interact with stabilized β -catenin to either modify Tcf factors and/or stimulate the recruitment of core transcriptional machinery to activate target gene transcription (Bienz and Clevers, 2003; Chan and Struhl, 2002). Irrespective of mechanism, demonstrated targets of Lef/Tcf- β -catenin activation regulate diverse processes such as tumor formation (Korinek et al., 1997; Morin et al., 1997), tissue homeostasis (van de Wetering et al., 2002) and stem cell maintenance (Reya et al., 2003), placing Tcf/Lef factors at the center of a number of crucial steps in development.

Tcf/Lef proteins can also function to repress the transcription of target genes (Brannon et al., 1999; Brantjes et al., 2001). Although poorly documented in mammals because of the lack of bona fide targets of repression, Tcf/Lef proteins can physically interact with co-repressor proteins such as CtBP and Groucho (Roose et al., 1998). In some cases, Wnt signaling has been shown to reverse repression. Whether Tcf/Lef

repression can be alleviated by non-Wnt mechanisms is unknown.

The human and mouse genomes each contain four Tcf genes, which are differentially expressed but encode proteins with highly homologous DNA binding domains and β -catenin interaction domains (Korinek et al., 1998b; Travis et al., 1991; van de Wetering et al., 1991). Although a double knockout of *Lef1* and *Tcf1* indicates that some contexts allow certain Tcfs to share a degree of functional redundancy (Galceran et al., 1999), different Lef/Tcf family members do not always behave similarly when expressed in the same cell type. Indeed, in mouse skin *Lef1* appears to function with β -catenin to activate genes involved in hair cell differentiation (Gat et al., 1998; van Genderen et al., 1994; Zhou et al., 1995), but when transgenically expressed in the same cells, *Tcf3* appears to act as a repressor to specify an alternative cell fate (Merrill et al., 2001).

In the developing mouse embryo, anteroposterior (AP) axis formation initiates during gastrulation beginning at embryonic day 6.5 (E6.5), when ectodermal cells acquire different fates: at the posterior embryonic/extra-embryonic border (EEX), an epithelial-mesenchymal transition occurs to form the mesoderm germ layer at the primitive streak region. The primitive streak expands distally, and a special group of cells at the anterior primitive streak (APS) form the axial mesoderm, which gives rise to the embryonic organizer, i.e. node, which is both necessary and sufficient to induce the AP axis

(Beddington, 1994). Analogous embryonic organizers in other animals are also necessary and sufficient to induce the primary embryonic axis, either the AP axis (Hensen's node in avians) or the DV axis (Spemann's organizer in amphibians, the embryonic shield in fish) (Beddington, 1994; Harland and Gerhart, 1997; Hensen, 1876). Further patterning within the mesoderm yields other, non-axial populations (e.g. lateral and paraxial mesoderm), which produce somites and other mesodermal structures.

In mouse, *Wnt3* is expressed at the appropriate time and location to promote primitive streak induction, and *Wnt3*^{-/-} embryos fail to undergo gastrulation (Liu et al., 1999). Similarly, β -catenin-null embryos also fail to specify an AP axis (Huelsen et al., 2000). Ectopic activation of Wnt signaling in early mouse embryos either by mutations affecting *Axin* or *Apc*, negative regulators of β -catenin stability, or by transgenic expression of *Wnt8c* all lead to ectopic AP axis specification and formation of multiple nodes (Ishikawa et al., 2003; Popperl et al., 1997; Zeng et al., 1997). Thus, Wnt signaling appears to be both necessary and, in some circumstances, sufficient for AP axis specification and formation of the node in developing mouse embryos.

Despite the proven requirement for upstream members of the Wnt signaling pathway, the role of specific Lef/Tcf proteins in mouse AP axis and node formation has remained unclear. As judged by gene targeting, ablation of *Tcf1*, *Tcf4* or *Lef1* results in either viable or neonatal lethal pups, without consequence to early embryonic development. The *Tcf1*^{-/-} *Lef1*^{-/-} double knockout embryos form excess neural ectoderm at the expense of paraxial mesoderm, as well as multiple neural tubes in the tail (Galceran et al., 1999). Although the *Tcf3* locus has not yet been targeted for mutation in any organism, in zebrafish morpholino knockdown of both *Tcf3* homologs (*Hdl* and *Tcf3b*) results in postgastrulation defects in neural patterning and anterior neural truncations (Dorsky et al., 2003; Kim et al., 2000). All of these effects in the *Tcf1*^{-/-} *Lef1*^{-/-} mice and the *hdl*-*tcf3b*- zebrafish, however, occur after the induction of the primary embryonic axis and after the formation of the embryonic organizer has already occurred. Interestingly, the antisense RNA-mediated knockdown of maternal and zygotic *Xenopus* XTcf3 leads to a markedly different phenotype characterized by the expansion of organizer cell fates and dorsoanteriorization of embryos (Houston et al., 2002). However, a similar role for mammalian Lef/Tcf proteins in either organizer formation or axis induction has yet to be identified.

Taken together, the findings to date suggest that either (1) additional Lef/Tcf functional redundancy accounts for the role of Wnt signaling in axis and node specification, (2) mouse Lef/Tcf proteins do not play a role in this process as they appear to do in *Xenopus* or (3) *Tcf3*, the lone Lef/Tcf family member left to be targeted in mice, is the crucial Lef/Tcf member in this process. Interestingly, *Tcf3* is expressed throughout the mouse embryo at E6.5, prior to primitive streak formation (Korinek et al., 1998b), which makes *Tcf3* a prime candidate to be either a positive or a negative regulator of Wnt-mediated AP axis specification. We have now tested this hypothesis directly by generating a null mutation in the murine *Tcf3* gene, and examining the consequences to Wnt signaling and early mouse embryogenesis. Our results reveal an essential and unique role for mouse *Tcf3* in restricting AP axis induction

during the onset of gastrulation. Similar to its *Xenopus* and zebrafish homologs, mouse *Tcf3* appears to function by repressing target genes in the early embryo.

Materials and methods

Generation and genotyping of *Tcf3*^{-/-} mice

Standard molecular biology techniques were used to construct the targeting vector (Fig. 2A). Briefly, a BAC clone containing the 5' region of *Tcf3* was isolated from the Genome System library Down to The Well system, and a 6kb *XbaI* fragment was subcloned into pBSK (Stratagene). The 3' arm of the vector [a 3 kb *XhoI* (blunted)-*SacII* fragment] was inserted into the *NotI* (blunted)-*SacII* digested pGKneobpAloxX2 PGKDTA vector kindly provided by Dr Phil Soriano (Seattle). PCR was used to insert a *BglII* site between exon 1 and 2, into which annealed oligos containing a loxP site were inserted. This loxP containing fragment (1.7 kb *PvuII*-*XhoI* fragment) was used as the 5' arm and it was ligated into *HincII*-*SacII* sites to complete the construction of the targeting vector. Fragments that were amplified by PCR were sequenced prior to usage.

The targeting vector was digested with *NotI* and electroporated in GS-1 ES cells (Sv/129 background; Genome Systems). Approximately 300 primary clones were screened by PCR, and Southern blotting was used to determine if faithful homologous recombination occurred in PCR-positive clones (Fig. 2B). A CMV-Cre recombinase expression plasmid was then transiently transfected into two separate '*Tcf3*^{+/neo}' clones, and 300 additional clones were isolated and genotypes for either loss of 'neo' only or loss of 'neo' and exon 2 to produce the *Tcf3*^{+/-} cells. Primers used for genotyping described in Fig. 2C are: 'rev', 5'-tcgccaagtgtaagtccttccc-3'; and 'for', 5'-agtgcctcctgtcaacgaatcgg. Two independent clones *Tcf3*^{+/-} ES clones were injected into recipient C57Bl6 blastocysts to produce male chimeras that were selected for mating with normal C57Bl6 females to obtain *Tcf3*^{+/-} mice.

Embryo in situ hybridization, immunofluorescence and histology

The age of embryos was determined based on the time of day harvested assuming noon on the day of plug discovery corresponds to day 0.5. For E6.5-E7.5 embryos staging criteria described (Downs and Davies, 1993) were used to determine the stage of gastrulation of embryos.

In situ hybridization was performed essentially as described (Wilkinson and Nieto, 1993). Briefly, embryos were fixed overnight in 4% PFA at 4°C, dehydrated in a graded methanol series and stored at -20°C in 100% methanol until in situ hybridization was performed. Embryos were then rehydrated, bleached in methanol/H₂O₂ (4:1) for 1 hour, washed in PBT, treated with proteinase K (2-3 minutes E7.5, 4-5 minutes E8.5), post-fixed in 4% PFA/0.2% glutaraldehyde, and hybridized with digoxigenin-labeled cRNA probes. Hybridized cRNA probes were detected with sheep anti-DIG AP FAB antibody (Roche). After BCIP/NBT (Roche) reaction to detect signal, embryos were dehydrated through a graded methanol series to develop the purple colored precipitate, rehydrated and cleared in 50% glycerol prior to imaging. Embryos were identified as *Tcf3*⁺ or *Tcf3*^{-/-} after imaging by digesting embryos in proteinase K and PCR as described above. Probes used in this study were specific for *Hex1* (P. Thomas), *En1* (A. Joyner), *Krox20* (*Egr2* - Mouse Genome Informatics) (D. Wilkinson), *Six3* (G. Oliver), *Foxa2* (E. DeRobertis) and brachyury (D. Wilkinson).

Immunofluorescent detection of proteins was performed on PFA-fixed, frozen sections as described previously (Merrill et al., 2001) with the following antibodies: guinea pig anti-Tcf3 (Merrill et al., 2001), mouse anti- β -catenin (Sigma) and rat anti-E-cadherin (M. Takeichi). Secondary antibodies, FITC or Texas Red-conjugated donkey antibodies (Jackson Labs) were used at 1:200 dilution.

Scanning electron microscopy (SEM)

SEM procedures were performed essentially as described (Sulik et al., 1994). Embryos were fixed overnight at 4°C in 2.5% glutaraldehyde and post-fixed in 2% osmium tetroxide for 2 hours. They were dehydrated in a graded series of ethanol. Crucial point drying and sputter coating with palladium/gold was used to preserve structures and highlight surface features. Embryos were mounted on metal stubs exposing the ventral/distal surface for optimal viewing of the node. Imaging was performed with a JEOL microscope.

Results

Activation of Wnt signaling and Tcf3 protein expression during gastrulation

Knockout mice lacking the gene(s) for *Tcf4*, *Tcf1*, *Lef1* or *Lef1* and *Tcf1*, all maintain the formation of the primitive streak and node, whereas ablation of either *Wnt3* or β -catenin prevents the formation of the primitive streak (Galceran et al., 1999; Huelsken et al., 2000; Korinek et al., 1998a; Liu et al., 1999). The lack of defects in Lef/Tcf mutant gastrulae raises the possibility that Lef/Tcf- β -catenin complexes may not be active at these early stages of gestation and suggest the possibility that stabilized β -catenin may be exerting its effects independently of Lef/Tcfs. If Lef/Tcf proteins do play a role in mouse AP axis formation, then the activation or de-repression of Lef/Tcf target genes would be expected to accompany Wnt expression.

To address this issue, we first assessed whether Tcf/Lef/ β -catenin regulated target genes are activated in the early mouse embryo with the TOPGal transgenic reporter, which is responsive specifically to Tcf/Lef/ β -catenin complexes (DasGupta and Fuchs, 1999). The first signs of TOPGal activity were seen at E6.5-E7.0, where X-Gal staining was detected beginning at the early streak (ES) stages of gastrulation [Fig. 1; for details of staging criteria for gastrulating embryos, see Downs and Davies (Downs and Davies, 1993)]. β -Galactosidase activity concentrated along the forming primitive streak (ps) region extending along both sides of the posterior EEX border (Fig. 1A) and was subsequently expanded distally in late streak (LS; Fig. 1B) and neural fold stages (Fig. 1C,D). These results were consistent with those previously reported for the BAT-Gal Wnt reporter transgene (Maretto et al., 2003) Sagittal sections of TOPGal stained neural fold stage embryos revealed activity in ectodermal and mesodermal cell types in the primitive streak region (Fig. 1E) and activity in the posterior half of the ventral node (Fig. 1E').

Next, we assessed whether Tcf3, the only Tcf/Lef member not previously targeted in knockout mice, could be a candidate to affect primitive streak or node formation. Previous studies indicated that *Tcf3* mRNA is expressed at E6.5 and then begins to decline in following days of gestation (Korinek et al., 1998b). To detect expression of Tcf3 protein at these stages, we conducted immunofluorescence microscopy on sectioned E6.5 to E7.5 embryos encapsulated by their deciduas. As judged by a monospecific Tcf3 antibody (Merrill et al., 2001), Tcf3 expression preceded gastrulation (Fig. 1F). At this early stage, Tcf3 was restricted to the nuclei (purple) of the ectodermal cells of the developing embryo. Analyses of sagittal and serial transverse sections showed that Tcf3 was present in the embryonic ectoderm throughout the proximodistal length (data not shown).

As mesoderm formed at the primitive streak region, the pattern of Tcf3 expression changed dramatically (Fig. 1G-I). Tcf3 immunoreactivity was weak or absent in the primitive streak, while it became intense in the ectoderm and mesoderm anterior to the node. (Fig. 1G). By E7.5, Tcf3 was also detected in a portion of the anterior endoderm. Thus, whereas the E6.5 embryo displayed relatively uniform anti-Tcf3 staining, the E7.5 embryo displayed an anterior gradient of Tcf3 immunoreactivity, with the transition at or near the node (Fig. 1I). Overall, reduction of Tcf3 protein in the posterior of the E7.5 embryos preceded the activation of TOPGal. Intriguingly, the earliest activation of TOPGal at E6.5 preceded Tcf3 downregulation.

Targeted ablation of *Tcf3* in ES cells and in mice

If Tcf3 functions prior to gastrulation, then it might be expected to act in concert with early Wnt signaling to affect the formation and patterning of the primitive streak. If, however, the function of Tcf3 does not occur until after the formation of the AP axis, then based on the retention of Tcf3 in the anterior of the gastrula, Tcf3 might be expected to act in patterning the anterior of the embryo, similar to the functions previously revealed for *Tcf3b* and *Hdl* (a truncated Tcf3 gene) in zebrafish development.

To distinguish between these possibilities, we created a null mutation in the *Tcf3* gene in mice. The 64 bp exon 2 of the *Tcf3* gene was targeted for excision, so that if the resulting *Tcf3* mRNA lacking exon 2 were stable, it would contain a frameshift and an early termination codon. Such nonsense-mutation containing mRNAs are typically unstable and rarely translated into protein (Wilkinson and Shyu, 2002). Moreover, previous mice containing potential truncation mutations residing much further downstream in the *Tcf1*, *Tcf4* and *Lef1* genes have not caused dominant negative effects (Korinek et al., 1998a; van Genderen et al., 1994; Verbeek et al., 1995).

The targeting vector was designed to provide flexibility in engineering either embryonic stem (ES) cells lacking exon 2, or ES cells harboring a floxed exon 2 for conditional knockouts (Fig. 2A). For the present study, we focused on the straight knockout. Shown in Fig. 2B are representative examples of the Southern blot analyses of ES cell genomic DNA, revealing a 5.9 kb *HinCII* fragment diagnostic for the floxed PGK-Neo cassette between exons 2 and 3 of the *Tcf3* gene, and a 3.3 kb *BglIII* fragment revealing the presence of the loxP site and new *BglIII* site inserted between exons 1 and 2 of the *Tcf3* gene (+/*neo*). After transfection with CMV-Cre plasmid, the loss of the PGK-Neo cassette was confirmed by Southern blot (+/- in Fig. 2B), and PCR verified the loss of the 170 bp exon 2 fragment (Fig. 2C).

From 26 litters involving two *Tcf3*^{+/-} heterozygote parents, 60 mice (36%) were *Tcf3*^{+/+} and 104 mice (64%) were *Tcf3*^{+/-}, as judged by PCR analyses (data not shown). These animals appeared normal, indicating no dominant-negative or haploinsufficiency defects from the single *Tcf3* allele alteration. However, between newborn and E11.5, no intact *Tcf3*^{-/-} embryos were found, suggesting that the loss of Tcf3 resulted in early embryonic lethality.

The first intact *Tcf3*^{-/-} embryos were recovered from three E9.5 litters (8^{+/+}, 20^{+/-} and 6^{-/-}), although they were only 20-40% the size of wild-type littermates. Although a beating heart and somites were present in some E9.5 *Tcf3*^{-/-} embryos,

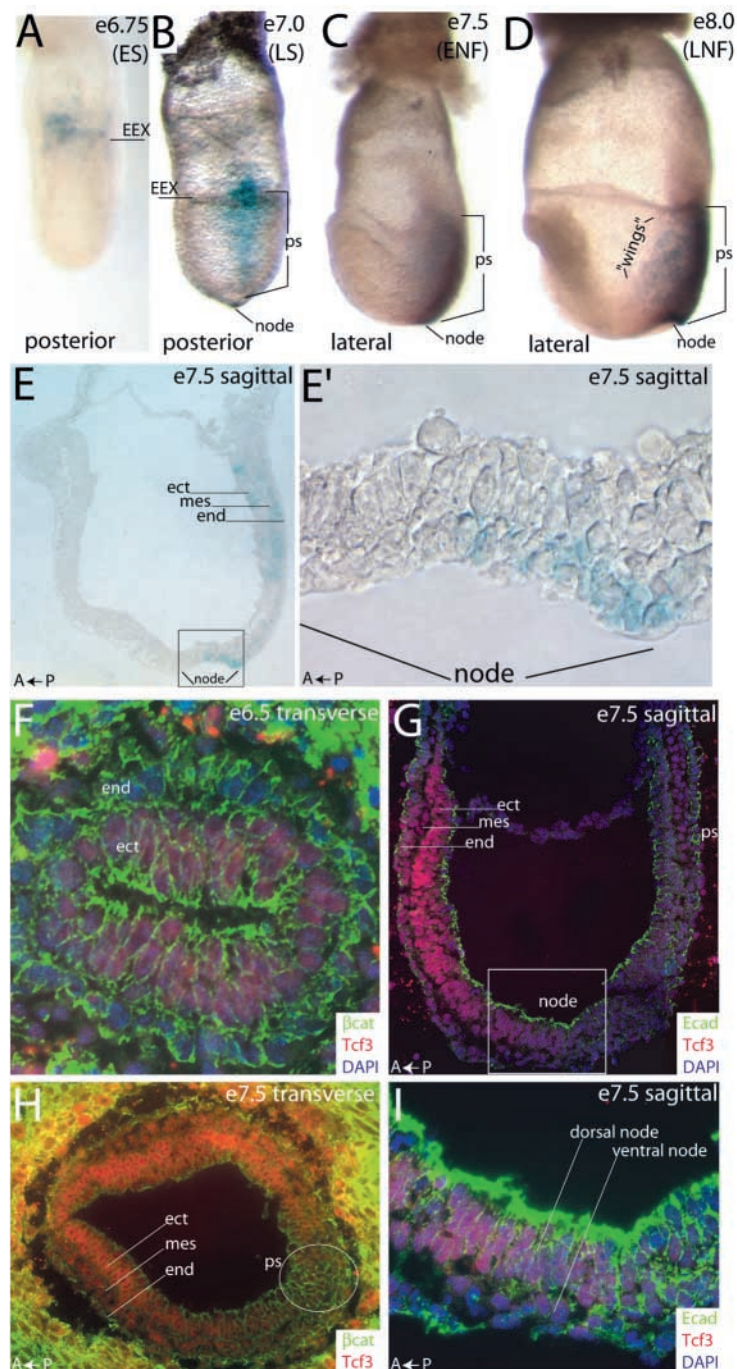


Fig. 1. Activation of Wnt target genes and expression of Tcf3 during gastrulation. (A-E') Tcf/Lef- β -catenin transcriptional activation revealed by X-gal staining of TOPGal transgenic embryo. The stage of gastrulation (Downs and Davies, 1993) is indicated in the top right-hand corner; the view displayed is indicated in the lower left-hand corner. The direction of posterior (P) to anterior (A) is indicated by an arrow. Boxed regions are those shown at higher magnification. TOPGal activity marks the posterior EEX border at the onset of gastrulation (A) and remains in the primitive streak region throughout gastrulation. (C-E') Neural-fold staged embryos express TOPGal in the primitive and the node. (E,E') Sagittal sections of TOPGal-stained embryos shows expression in both ectodermal and mesodermal cell types and in the posterior cells of the ventral node. (F-I) Indirect immunofluorescence microscopy with antibodies displayed in the lower right-hand corner (color coded according to the secondary antibody used for detection) and embryo sections of the age and plane of sectioning displayed in the upper right-hand corner. (F) Tcf3 (red) is expressed throughout the embryonic ectoderm before primitive streak induction, and (G,H) diminished posteriorly during gastrulation. (I) Close inspection of the node reveals a gradient of Tcf3 expression rising in concentration from the posterior to the anterior of the node. ES, early streak stage; LS, later streak stage; EEX, embryonic/extra-embryonic border; ENF/LNF, early/late neural-fold stage; end, endoderm; mes, mesoderm; ect, ectoderm; ps, primitive streak.

folds extend anteriorly past the developing heart, and forebrain, midbrain and hindbrain regions are identifiable (Fig. 3A').

All E8.5 *Tcf3*^{-/-} embryos were unmistakably aberrant, although morphological abnormalities exhibited variable penetrance in a range from mild (48%; Fig. 3B-D) to severe (52%; Fig. 3E-F'). Most striking in the mildly affected *Tcf3*^{-/-} embryos was the duplication of developing neural-folds (Fig. 3B,B'). Although the appearance of supernumerary neural-folds was most common in the anterior of *Tcf3*^{-/-} embryos, their pattern and structure were variable. Histological staining of semithin transverse sections through the neural folds revealed that instead of a single neural groove as in wild-type embryos (Fig. 3G), multiple neural grooves and abundant neurectodermal cells were present in *Tcf3*^{-/-} embryos (Fig. 3H). In mildly affected E8.5-E9.5 *Tcf3*^{-/-} embryos, somites were often visible along the AP midline, and occasionally an extra row was observed (asterisks in Fig. 3C,C'). These data showed that Tcf3 is not required for the generation of paraxial mesoderm or its condensation into somites.

Mildly affected embryos also frequently displayed an enlarged heart (Fig. 3B'), and all embryos displayed anterior truncations (Fig. 3B',D compare with 3A').

Although supernumerary neural-folds were a hallmark of mildly affected E8.5 *Tcf3*^{-/-} embryos, these structures were grossly runted or absent in severely affected embryos, which also failed to produce somites and heart (Fig. 3E,F). However, consistent with the presence of multiple neural folds in mildly affected mutants, multiple grooves (ng) along the ventral surface were evident in the severely affected mutants (Fig. 3E). These grooves extended along the anterior half of the embryo, which was frequently bent laterally. Distally, the severely affected embryos frequently exhibited atypically large areas

anterior neural structures were conspicuously absent (not shown). At E8.5 and earlier, *Tcf3*^{-/-} embryos were recovered at Mendelian ratios and no signs of excessive resorption were noted. PCR analyses confirmed the existence of the *Tcf3* mutation and loss of the *Tcf3* wild-type allele (Fig. 2C), and anti-Tcf3 immunoblot analysis confirmed the loss of Tcf3 protein in E8.5 *Tcf3*^{-/-} embryos (Fig. 2D).

Morphological defects in *Tcf3*^{-/-} embryos

Just after gastrulation at e8.5, *Tcf3*^{+/+} and ^{+/-} embryos (WT) had well-established AP axial structures, distinct neural-folds, somites and a heart (Fig. 3A,A'). The rostral ends of the neural-

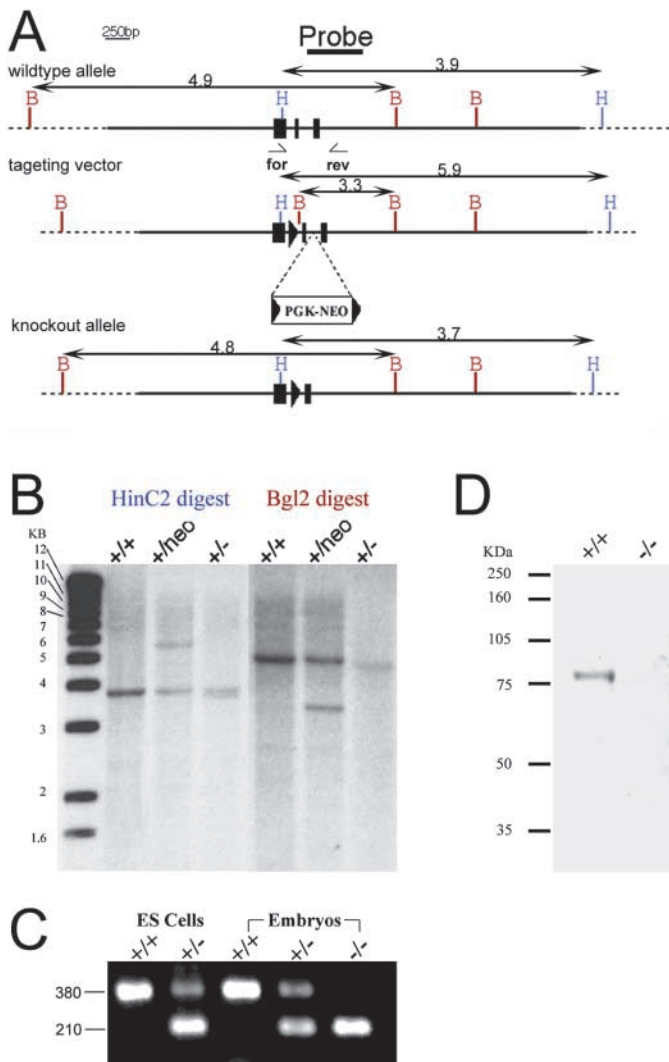


Fig. 2. Generation of *Tcf3*^{-/-} mice. (A) Targeting strategy. Exons 1-3 of *Tcf3* are shown as boxes along the unbroken line representing the *Tcf3* gene fragment present in the targeting construct. Broken lines represent *Tcf3* gene fragments flanking the targeting construct. The numbers above double-sided arrows represent the size in kb of the fragments generated by digestion with either *Bgl*II (B) or *Hinc*II (H). The triangles between exons 1 and 2 and flanking the PGK-NEO cassette represent loxP sites for Cre-mediated recombination. Small single-sided arrows depict the position of forward (for) and reverse (rev) PCR primers used for genotyping of mice. (B) Homologous recombination events in ES clones were confirmed by Southern blotting. +/+, ES cells prior to electroporation; +/neo, one ES clone that had correctly integrated the targeting vector fragment into the *Tcf3* locus; +/-, a clone derived from the +/neo clone after electroporation with Cre-recombinase was used to remove the PGK-NEO cassette and exon 2 of *Tcf3*. (C) Genotyping reaction with primers shown in A shows the loss of one copy of exon 2 in *Tcf3*^{+/-} ES cells and mouse embryos, and the loss of both copies of exon 2 in *Tcf3*^{-/-} embryos. (D) Western blot of total protein from E8.5 embryos with an antibody directed towards the C terminus of Tcf3 protein confirms loss of Tcf3 protein in *Tcf3*^{-/-} embryos.

that appeared to lack underlying ectoderm or mesoderm (Fig. 3E,F', red arrows). The significance of these regions is delineated below.

The earliest recognizable defects were detected in E7.5 *Tcf3*^{-/-} embryos, where a frequent bulging and less frequent duplication of the primitive streak were detected (Fig. 3I). Histological examination of these morphological perturbations revealed an aberrant accumulation of mesoderm (Fig. 3I). Overall, these data were consistent with defects involving partial and sometimes complete duplications of AP axis structures, including neural grooves and primitive streaks. Other abnormalities, including enlarged cardiac sacs, multiple large blood vessels (v) and foregut defects (fg) seemed to be secondary consequences of partial AP axis duplication. We pursue this avenue in greater detail below.

Defective neural patterning in *Tcf3*^{-/-} embryos

The forebrain defects in postgastrulation E8.5 *Tcf3*^{-/-} embryos bore a strong resemblance to those seen upon ectopic activation of Wnt signaling (Mukhopadhyay et al., 2001; Popperl et al., 1997), and in *hdl*, *tcf3b* knock-down zebrafish embryos (Dorsky et al., 2003; Kim et al., 2000). To explore the extent to which these later stage defects might resemble artificial Wnt activation, we examined the expression of neural-specific genes in E8.5 embryos. Fig. 4 illustrates representative whole-mount in situ hybridization performed on groups of ~10 E8.5 embryos (6-9 *Tcf3*^{+/+} or ^{+/-} and 3-4 *Tcf3*^{-/-}). Data for ^{+/+} or ^{+/-} embryos were indistinguishable and are referred to as 'wild-type'.

As expected, well-known forebrain-specific markers, such as *Hexs1*, *Six3* and *Bf1* mRNAs, were expressed in the anterior neuroectoderm of WT E8.5 embryos (data shown for *Hexs1* in Fig. 4A,A'). In mutant embryos, expression of these mRNAs was markedly reduced. Of the three markers examined, the only definitive expression of forebrain markers was for *Hexs1*, and this was weak and only detected in the rostral neuroectoderm of the most mildly affected *Tcf3*^{-/-} animals (Fig. 4B,B').

Perturbations were also detected in midbrain and hindbrain gene expression. *En1* is typically expressed in neuroectoderm at the caudal end of the midbrain (Fig. 4C,C'). In mutant embryos, *En1* was expanded rostrally, and its distance from the rostral tip of the embryo was shortened, consistent with the severe reduction of the forebrain (compare bar in Fig. 4C to bar in Fig. 4D). Frontal views revealed that neuroectoderm retained *En1* expression but did not develop a neural groove (Fig. 4D') like wild-type embryos did (Fig. 4C'). For the hindbrain marker *Krox20*, wild-type embryos exhibited robust expression in rhombomeres 3 and 5 (Fig. 4E,E'), whereas *Krox20* expression in knockout embryos was restricted to a single band on each neural fold, and was markedly reduced in intensity (Fig. 4F,F'). Additionally, rather than being confined to the neural groove, *Krox20* was detected on the lateral surfaces of *Tcf3* mutant neural-folds (Fig. 4F'). Thus, loss of Tcf3 not only resulted in a failure to specify the most rostral neuroectoderm, but also more broadly caused abnormalities in caudal brain regions.

Multiple nodes and notochords in *Tcf3*^{-/-} embryos

Defects in early patterning events that produced duplications and expansions of axial structures in *Tcf3*-null mouse embryos had not been observed in the morpholino knockdowns of Tcf3 gene expression in zebrafish. By contrast, gross expansion of Spemann's organizer was observed in knockdown of XTcf3

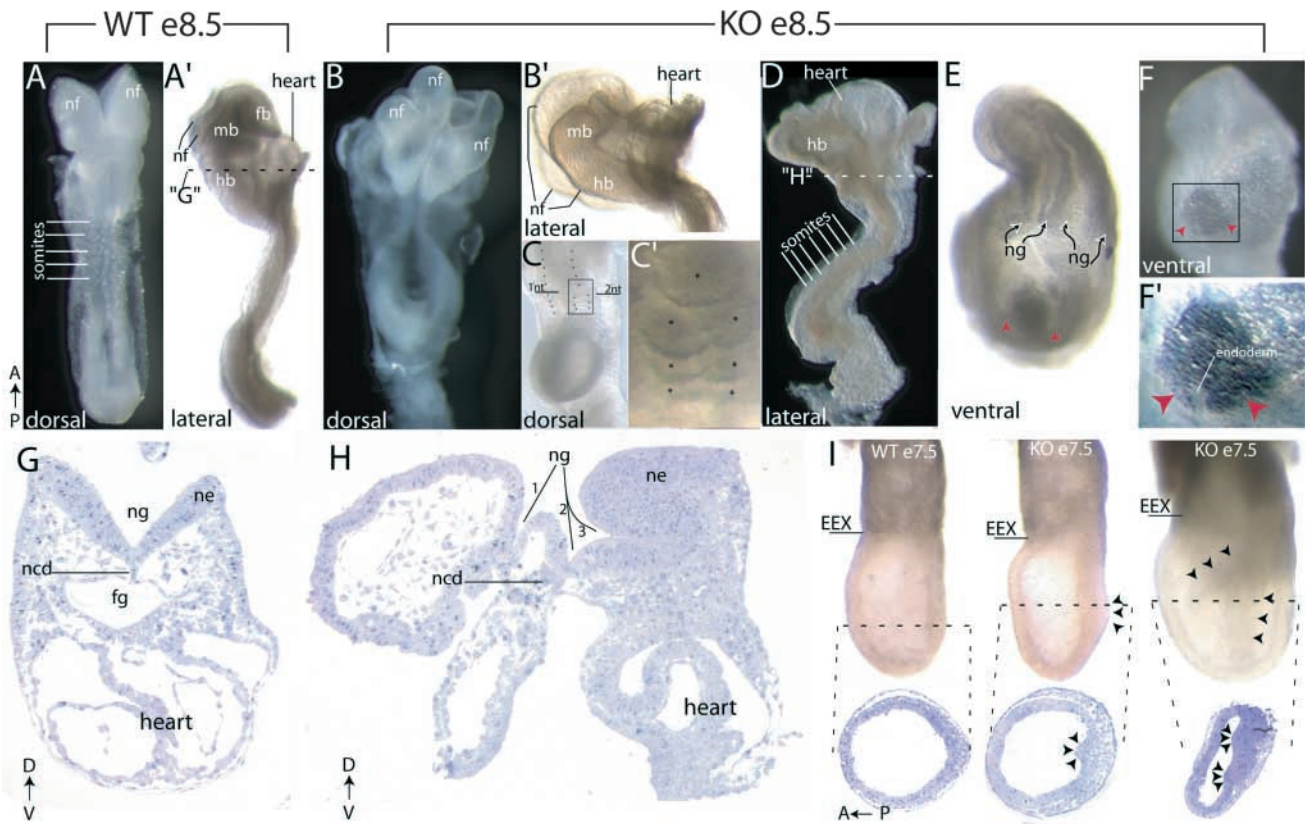


Fig. 3. Morphological defects in *Tcf3*^{-/-} embryos. (A-F') Wild-type (WT; A,A') and *Tcf3*^{-/-} (KO; B-F') E8.5 embryos. The view displayed is indicated in the lower left-hand corner. (A,A') Wild-type embryos display bilateral symmetry with two neural-folds (nf) and somites along either side of the AP axis. Rhombomere formation in the neural-folds allows identification of forebrain (fb), midbrain (mb) and hindbrain (hb) regions. The broken line in A' refers to the position of the section displayed in G. (B-D) Mildly affected *Tcf3*^{-/-} embryos display multiple morphological defects. (B,B') Multiple neural-folds are clearly visible in some mutants. (C) Caudal half of a *Tcf3*^{-/-} embryo with a secondary neural tube (2^{nt}) and extra row of somites (asterisks) adjacent to the primary neural tube (1^{nt}) which runs along the primary AP axis. A higher magnification view of the boxed region in C is displayed in C'. (D) Lack of forebrain structures and an enlarged heart appear in the *Tcf3*^{-/-} mutant shown. Broken line in D refers to the position of the section displayed in H. (E-F') Ventral views of severely affected *Tcf3*^{-/-} embryos. (E) Multiple neural groove-like structures (ng) are apparent along the ventral surface of the *Tcf3*^{-/-} embryo but neural-folds appear to be absent. Red arrowheads indicate areas along the ventral surface that appear to lack underlying mesoderm and ectoderm. The boxed region in F is shown in higher magnification in F'. (G,H) Toluidine Blue stained semithin sections of embryos in A' and D, respectively. Notice the single neural-groove in G and the three neural grooves in H. (I) E7.5 wild-type or knockout embryos, as indicated at the top of each embryo. A Toluidine Blue stained semithin section from the plane indicated with the broken line is displayed below each embryo. Notice the morphological defects in the primitive streak region of *Tcf3*^{-/-} embryos manifest either a bulge (arrowheads, middle embryo) or a second primitive streak region (arrowheads, right embryo). ncd, notochord; ne, neuroectoderm; fg, foregut, EEX, embryonic/extra-embryonic border.

from *Xenopus* embryos, although distinct duplications of either the organizer or the primary embryo axis in XTcf3⁻ embryos were not reported (Houston et al., 2002). Given the importance of the node and notochord in postgastrulation patterning of axial structures, the appearance of expanded or duplicated nodes and notochords in *Tcf3*^{-/-} embryos could explain many of the observed morphological defects. Therefore, we next addressed whether the node and notochord were duplicated and/or expanded in *Tcf3*^{-/-} embryos.

Towards the end of gastrulation (E7.5), node and notochord are readily visible by scanning electron microscopy (SEM) as an indented club-like structure on the embryo surface (Fig. 5A). In the normal embryo, the ventrally located node is most obvious, and is composed of small, rounded, monociliated progenitor cells (Fig. 5A,A'; green arrow). Arising anterior of the node, the derivative cells of the notochord are similar in appearance, forming a structure that is two to three cells wide (double blue

arrows in Fig. 5A). Both the node and the notochord are readily distinguished from the surrounding, more superficial endodermal cells, which are flatter and larger in appearance.

The organization of node and notochord cells within severely affected E8.0 *Tcf3*^{-/-} embryos was strikingly abnormal. Two distinct nodes (green arrows) were separated by a thin strip of endodermal cells (red arrow) at the posterior of the structure (Fig. 5B-B'). These seemingly duplicated nodes merged rostrally, forming an expanded notochord-like structure along the ventral surface of the embryo (blue arrows in Fig. 5B). As the notochord-like structures extended rostrally (below the blue arrows in the example shown), they branched dorsolaterally into numerous streaks of what appeared to be notochord strands along the ventral surface of the mutant (boxed region in Fig. 5B, at higher magnification in B'). In some areas, the width of notochord-like structures was larger than that of the node of wild-type embryos.

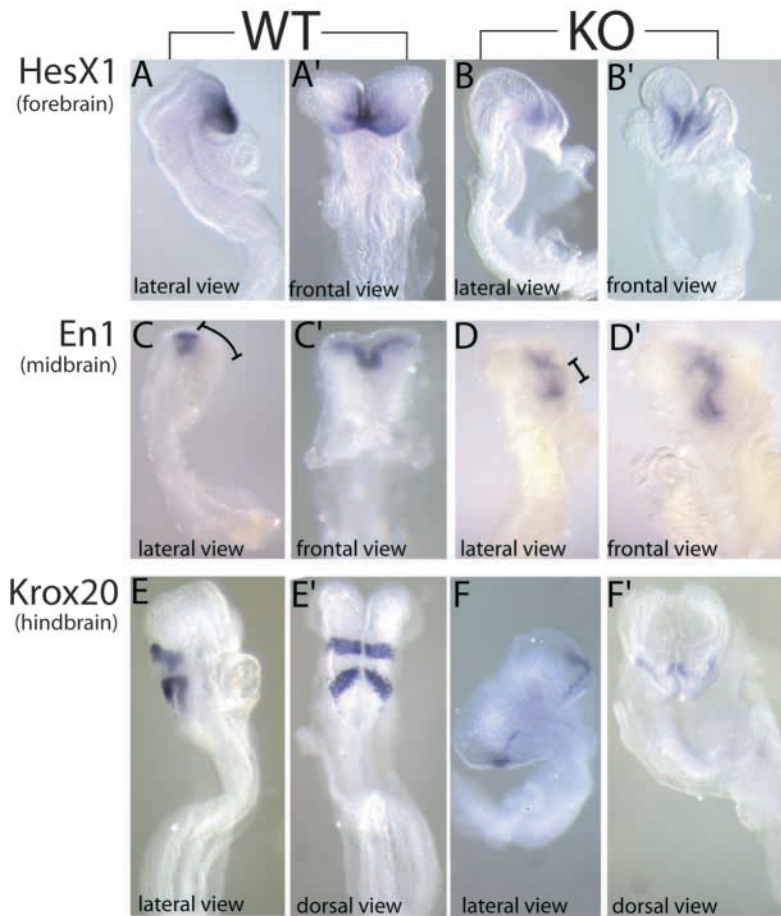


Fig. 4. *Tcf3*^{-/-} embryos display defective patterning of anterior neural regions. In situ hybridization of E8.5 wild-type (WT; A,A',C,C',E,E') and *Tcf3*^{-/-} (KO; B,B',D,D',F,F') embryos using cRNA probes as indicated. Wild-type embryos display prominent staining for *Hesx1* (A,A') in the forebrain whereas mutant embryos (B,B') display very weak *Hesx1* staining. (C,C') *En1* is expressed in the midbrain-hindbrain boundary caudal to the midbrain. The distance of expression to the rostral end of the embryo is marked by the curved bracket (C). (D,D') *En1* expression is observed in the mutant embryos, but the distance from the rostral end is diminished (bracket). Note also the deformed neural groove in mutant (D'). (E,E') Robust *Krox20* is present in rhombomeres 3 and 5 of the wild-type embryo. (F,F') Weak *Krox20* expression is observed in only one stripe of neuroectoderm in the mutant embryos. In addition, the expression of *Krox20* is expanded laterally compared with the pattern seen in the wild type.

To assess whether these node-like and notochord-like structures exhibited molecular characteristics of organizer cell populations, we examined a pair of marker genes, *brachyury* and *Foxa2*, which are important for organizer function at this stage. In wild-type embryos, *brachyury* is expressed in the primitive streak and then concentrates in the node and notochord (*ncd*) (Fig. 5C,C'). In *Tcf3*^{-/-} embryos, *brachyury* was often grossly expanded (Fig. 5D,D'). These patterns varied, but were a direct reflection of the degree of expanded/duplicated node and notochord cells in a given *Tcf3*^{-/-} embryo. In the most severely affected embryos, *brachyury* expression nearly covered the entire ventral surface. Similar findings were obtained with *Foxa2*. In wild-type embryos, *Foxa2* is expressed in the node and notochord as well as in the neural floor plate when dorsoventral polarity is established in the neural tube (Fig. 5E,E'). In mutant embryos, *Foxa2* expression was considerably broader and variable, but always reflective of the morphological expansions and duplications/multiplications of node and notochord (Fig. 5F,F').

The use of *Foxa2* and *brachyury* as markers in E8.5 embryos provided graphic illustrations of the various different axis defects observed in our *Tcf3*^{-/-} embryos. The most striking were cases where the axis duplications appeared to occur on opposite sides of the embryo (Fig. 5G,G').

Mesodermal patterning defects in *Tcf3*^{-/-} gastrulae

To begin to elucidate the causes of the AP axis duplications

and expansions of axial mesendoderm in *Tcf3*^{-/-} embryos, we examined molecular events known to be important for proper AP axis induction and subsequent patterning of the primitive streak mesoderm. The extra-embryonic organizer, anterior visceral endoderm (AVE), is required early to pattern the gastrulating epiblast for AP axis formation (for a review, see Lu et al., 2001). Expressed in the AVE, the Nodal inhibitors *Cer1* and *Lefty1* (*Lefta* – Mouse Genome Informatics) are crucial to this process, as judged by the AP axis duplications caused by expanded Nodal signaling in *Cer1*^{-/-} *Lefty1*^{-/-} embryos (Perea-Gomez et al., 2002).

To determine whether loss of *Tcf3* interferes with the ability of the AVE to restrict Nodal activity, we examined the expression of endodermal markers in *Tcf3*^{-/-} gastrulae. *Cer1* expression was detected in the AVE of all wild-type and *Tcf3*^{-/-} embryos examined, although it was expanded in the posterior endoderm of the mutant embryos (Fig. 6A-B'). An additional AVE marker, the homeobox gene *Hex*, was also largely unaffected in its expression (Fig. 6C,D). The intact expression of AVE markers indicated that the axis duplications are not caused by loss of Nodal antagonists in the AVE.

As the epiblast cells flow into the primitive streak region and form nascent mesoderm, the mesoderm is patterned to follow specific developmental fates. Axial mesoderm, which develops into node and notochord organizers, is specified early compared with the paraxial and lateral mesoderm (Kinder et al., 1999; Lawson et al., 1991). To assess whether the loss of *Tcf3* affects axial mesodermal patterning in early gastrulation, we examined the expression of a series of marker genes that specify early mesodermal populations. *Brachyury* is one of the first mesodermal markers that is normally expressed along the midline of the primitive streak region (Fig. 6E). In *Tcf3*^{-/-} embryos, *brachyury* was maintained in the primitive streak region. *Brachyury* staining either revealed a crooked or bent path in *Tcf3*^{-/-} embryos (Fig. 6F,F') (57% of mutants) or staining intensity was slightly diminished (28% of mutants; not shown). Normal *Cripto* (*Cfc1* – Mouse Genome Informatics) expression was detected in all wild-type and knockout embryos examined

Fig. 5. Duplications and expansions of node and notochord in *Tcf3*^{-/-} embryos. (A-B'') Scanning electron microscopy (SEM) images of the ventral surface of wild-type (WT; A, A') and *Tcf3*^{-/-} (KO; B, B'') embryos (anterior towards the lower left-hand corner). Arrows: Green, nodes; blue, notochords; red, endodermal strip. White line indicates notochord-endoderm boundary in B and B'. White boxes in A and B outline areas magnified in A' and B', respectively. Note the club-like structure of the single node and notochord in the wild-type embryo and the duplicated node and expanded notochord in mutant embryo. (C-F') Whole-mount in situ hybridizations of E8.5 wild-type and knockout embryos, probed with digoxigenin-labeled cRNAs for brachyury or *Foxa2* as indicated. Anterior is towards the top of each image. The three embryos in each panel in D and F show different representative aberrant patterns, reflective of the extent of node/notochord multiplication. Opposing arrowheads indicate thickness of notochords (ncd); arrows indicate splitting of the notochord, often seen in mutant embryos. (G, G') *Tcf3*^{-/-} embryo with a rostral extension probed for brachyury expression. Anterior is leftwards for both images. The primary primitive streak (1°PS) and a secondary primitive streak (2°PS) are positive for brachyury expression. Emerging from the secondary primitive streak are structures similar to a node (arrows) and notochord (arrowheads).

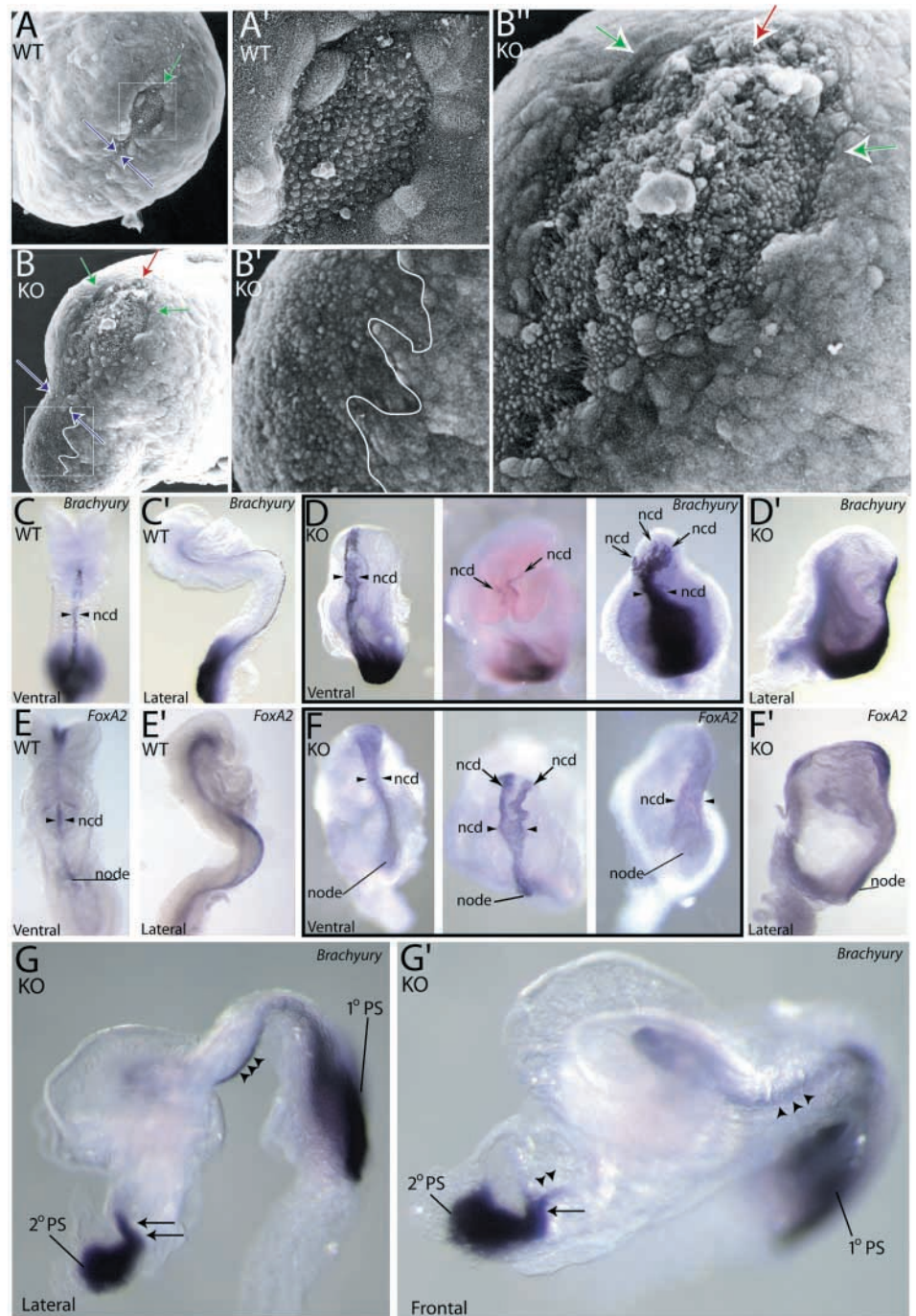


(Fig. 6G-H'). Overall, the pattern of these markers indicated that the loss of *Tcf3* did not result in gross defects in general mesoderm formation.

In E7.0 embryos, *Foxa2* is normally expressed in the axial mesoderm that forms the APS, where it is required for node formation (Ang and Rossant, 1994; Weinstein et al., 1994) (Fig. 6I). In 75% of the *Tcf3*^{-/-} embryos examined, *Foxa2* expression was altered in variable patterns (Fig. 6J, J'). In half of the *Tcf3*^{-/-} embryos, *Foxa2* expression was clearly expanded but still localized at its normal position at the distal tip of the primitive streak (Fig. 6J). In 25% of *Tcf3*^{-/-} embryos, signs of ectopic expression were visible

such as shown in Fig. 6J', where strong hybridization was seen along the perimeter of the extra-embryonic/embryonic border.

Complementary to the axial mesoderm of the anterior primitive streak, the lateral mesoderm is marked by expression of *Lefty2* (*Leftb* – Mouse Genome Informatics) (Meno et al., 1999) (Fig. 6K). Expression of *Lefty2* was diminished in most (78%) *Tcf3*^{-/-} embryos (Fig. 6L, L'). Concomitant with the reduction in *Lefty2* was a corresponding expansion of the region where axial mesoderm normally develops (area below the red line in Fig. 6K-L'). Together, these findings suggested that the loss of *Tcf3* results

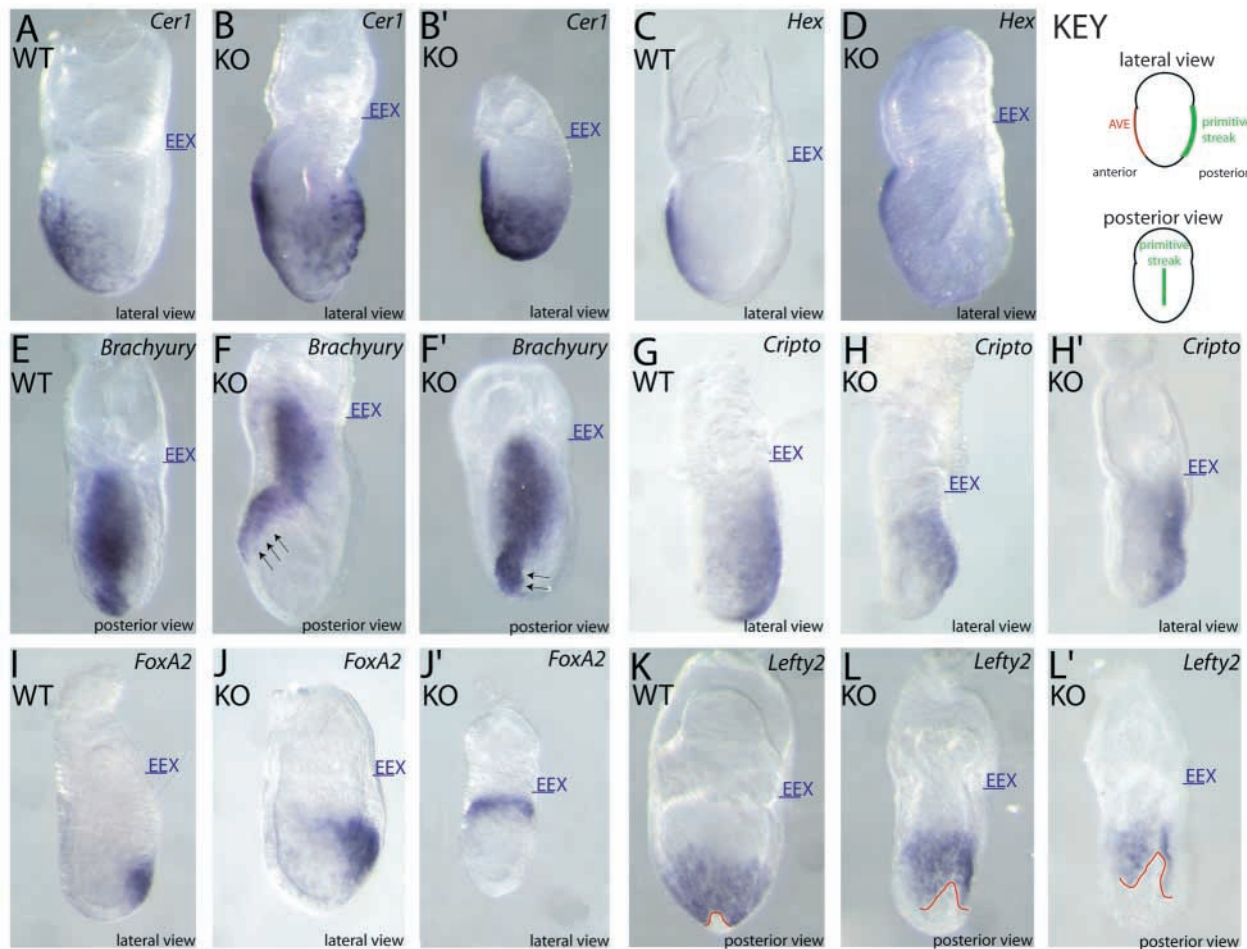


Fig. 6. Mesodermal patterning defects in *Tcf3*^{-/-} embryos. (A-L') In situ hybridization with wild-type (WT) or *Tcf3*^{-/-} (KO) E7.0 embryos using the probes indicated in the upper right of each panel. The view displayed is indicated in the lower right corner and embryos are positioned as indicated in the key. EEX marks the embryonic/extra-embryonic border. (A-D) Endodermal markers *Cer1* (A-B') and *Hex* (C,D) are maintained in *Tcf3*^{-/-} (B,B',D) embryos. (E-F') *Brachyury* marks the primitive streak and axial mesendoderm in the wild-type (E), and it is maintained in *Tcf3*^{-/-} embryos (F,F') but adopts a bent or twisted pattern (arrows) consistent with multiple primitive streaks. (G-H') *Cripto* expression is similar in wild-type (G) and *Tcf3*^{-/-} embryos (H,H'). (I-J') *Foxa2* expression marks the axial mesoderm of the APS in the wild type (I). In *Tcf3*^{-/-} embryos, *Foxa2* expression is either expanded (J) or ectopically expressed such as shown circumferentially along the EEX border in J'. (K) *Lefty2* is expressed in the lateral mesoderm and its pattern reveals a 'notch' (outlined in red) at the distal tip of the wild-type embryo, reflective of the axial mesoderm-mesendoderm. (L,L') In *Tcf3*^{-/-} embryos, *Lefty2* expression is diminished and reveals a larger 'notch' (outlined in red) indicating the increased axial mesoderm in the mutant.

in expansion of axial mesoderm at the expense of other mesodermal cell types.

TOPGal activity retains its expression pattern during gastrulation in *Tcf3*^{-/-} embryos

Based primarily on the VegT-dependent upregulation of organizer genes in XTcf3-depleted embryos, a function of XTcf3 in *Xenopus* gastrulae is to repress target genes activated by non- β -catenin dependent mechanisms (Houston et al., 2002). Consistent with this model in *Xenopus*, the removal of Tcf-binding sites from the *Siamois* promoter elevates its activity in ventral blastomeres of embryos (Brannon et al., 1997). These data from *Xenopus* combined with similarities between *Tcf3*^{-/-}, *Axin*^{-/-}, *Apc*^{neo/neo} and Wnt8c transgenic phenotypes together suggest that murine Tcf3 functions to repress target genes during induction of the AP axis (Ishikawa et al., 2003; Popperl et al., 1997; Zeng et al., 1997).

To evaluate whether Tcf3 mediates its non-redundant effects on early gastrulation through repression or activation of Wnt target genes, we mated the TOPGal transgenic mice on the *Tcf3*^{-/-} background, and examined TOPGAL expression in gastrulating embryos. If Tcf3 functions as a non-redundant activator of Wnt target genes, TOPGal activity should be absent from the *Tcf3*^{-/-} gastrula; if Tcf3 functions as a non-redundant repressor that normally counteracts other Lef/Tcf factors in Wnt-receiving cells, then this might be reflected in ectopic TOPGal expression. If the non-redundant role of Tcf3 is to suppress genes that require other factors for their transactivation, then TOPGal should be expressed only in the axial mesodermal cells and their progeny, which are normally TOPGal positive (see Fig. 1).

The results of this experiment are compiled in Fig. 7. TOPGal expression was clearly maintained in the *Tcf3*^{-/-} gastrula even at the early stages of primitive streak formation



Fig. 7. TOPGal expression patterns maintained in *Tcf3*^{-/-} embryos. TOPGal transgenic, wild-type (WT) or *Tcf3*^{-/-} (KO) embryos of the indicated stages of development were stained with X-gal to identify the location of activation of *Lef/Tcf*- β -catenin target genes. (A) Lateral view of a wild-type late streak embryo is weakly positive for TOPGal activity in the primitive streak region. (B,C) *Tcf3*^{-/-} embryos display TOPGal positive staining in the primitive streak region. The intensity of staining is indistinguishable from wild type. (D,D') Headfold staged *Tcf3*^{-/-} embryos display a TOPGal expression pattern indistinguishable from wild-type embryos (see Fig. 1C,D) and include positive TOPGal expression in the node. (E) Tail of a wild-type E8.5 embryo. TOPGal is present in the posterior node and the mesenchymal cells near the node. (F) *Tcf3*^{-/-} E8.5 embryo. TOPGal expression is found in the tail of the embryo. (F') Dorsal view shows a duplication of the node in this embryo. TOPGal is maintained in the same pattern as wild type in the node and the surrounding mesenchyme, despite the duplication.

(KO; Fig. 7B,C). Analogous to the pattern seen in wild-type embryos, X-gal staining was in the posterior of the embryo, at the EEX border. TOPGal expression was also detected in the primitive streak and node of embryos that had formed neural-folds (Fig. 7D,D'). Interestingly, even in embryos with a clearly duplicated node, TOPGal expression was still faithfully maintained in the correct, but now expanded, cell population (Fig. 7E-F'). As we failed to detect suppression, elevation and ectopic activation of TOPGal, these data best fit a model whereby the non-redundant role of *Tcf3* is as a

repressor of genes that are not activated by Wnt signaling alone.

Discussion

Despite the conclusion that both murine and zebrafish *Tcf3* act as transcriptional repressors, loss of murine *Tcf3* results in early gastrulation defects that are different from the postgastrulation headless phenotype caused by knockdown of zebrafish *hdl* and *pcf3b*. The mildly affected mouse mutants displayed anterior neural truncations and other neural patterning defects similar to the zebrafish knockdown experiments; however, the zebrafish experiments did not reveal a function for *hdl* or *pcf3b* in the formation of the AP axis or patterning of primitive streak mesoderm. Possible explanations for the differences include: (1) a maternal store of *hdl* or *pcf3b* which was not affected by morpholino-mediated knockdown; (2) the presence of an additional *Tcf*, such as maternally expressed *Tcf4*, in the early zebrafish embryo; or (3) an additional non-*Tcf* related mechanism by which zebrafish restricts AP axis formation.

Studies with XTcf3 knockdowns revealed greater similarities to our mouse knockout. Knockdown of XTcf3 causes an induction of dorsal blastomere-specific genes by a VegT-dependent mechanism (Houston et al., 2002). Many of the dorsal-specific genes upregulated by loss of XTcf3 are involved in formation of the Spemann organizer. In mouse *Tcf3*^{-/-} embryos, we also find expansions of node cells and the upregulation of *Foxa2*, a Nodal target gene required for specification of node cell types. However, *Tcf3*^{-/-} mouse embryos displayed distinct duplications of the AP axis not seen in the *Xenopus* knockdown embryos

Curiously, no other *Lef/Tcf* gene has been directly implicated in AP axis induction despite the requirement of *Wnt3* and β -catenin for this process (Huelsen et al., 2000; Liu et al., 1999). In mouse, *Lef1*^{-/-}, *Tcf1*^{-/-} and *Lef1*^{-/-} *Tcf1*^{-/-} embryos are all competent at inducing an AP axis, and *Tcf4* is not expressed in pregastrula embryos (Galceran et al., 1999; Korinek et al., 1998a; Korinek et al., 1998b). Our studies with TOPGal embryos provide evidence that *Wnt3* functions through *Lef/Tcf*- β -catenin activation of target genes during AP axis induction. Furthermore, the induction of the AP axis coupled with the persistence of TOPGal expression in *Tcf3* knockout embryos reveals a previously unrealized level of functional redundancy between *Lef/Tcf* factors in transducing this signal.

The putative redundant function of *Tcf3* in promoting AP axis induction in *Lef1*^{-/-} *Tcf1*^{-/-} embryos becomes particularly interesting when one considers its opposing, non-redundant function in early embryogenesis. The fact that TOPGal activity in *Tcf3* mutant embryos is both maintained in the expanded organizer cells and not ectopically expressed in other cells offers important insights into how *Tcf3* must be exerting its non-redundant effects. Together, these findings indicate that *Tcf3* acts alone in restricting the activation of target genes that are positively regulated by other transcription factors. The simplest model consistent with these data is that the primary function of *Tcf3* is essential for repressing the expression of genes that promote AP axis induction and formation of axial mesoderm.

Given the requirement for Nodal signaling during AP axis

induction (Conlon et al., 1994) and axial mesoderm patterning (Hoodless et al., 2001; Vincent et al., 2003; Yamamoto et al., 2001) and the VegT-XTcf3 interaction elucidated in *Xenopus* organizer formation (Houston et al., 2002), it is attractive to speculate that Tcf3 might be repressing transcriptional targets of Nodal signaling. In support of this model, ectopic primitive streak formation in chick embryos requires the combined action of both Wnts and a Nodal-like molecule, Vg1 (Skromne and Stern, 2001). As the transcriptional activation of *Foxa2* is directly downstream of Nodal signaling (Hoodless et al., 2001; Yamamoto et al., 2001), the ectopic expression of *Foxa2* in the gastrulating *Tcf3*^{-/-} embryo lends further support to this view. We also noted that a *Foxa2* promoter element harboring multiple, conserved Lef1/Tcf-binding sites directs transgenic expression in axial mesoderm and node (Sasaki and Hogan, 1996).

The phenotype of Tcf3 mutant embryos is similar to that reported for the loss of Axin or Apc, two other inhibitors of Wnt signaling (Ishikawa et al., 2003; Popperl et al., 1997; Zeng et al., 1997) and ectopic expression of Wnt8c (Popperl et al., 1997). Previously, these effects were attributed to the ectopic expression of target genes normally regulated by β -catenin/Tcf transactivating complexes. However, the lack of ectopic TOPGal activity in *Tcf3*^{-/-} embryos suggests that β -catenin/Tcf transactivating complexes are not required for the axis duplication phenotypes. An alternative mechanism consistent with our data is that Tcf3 functions as a transcriptional repressor in the absence of β -catenin, and that ectopic stabilization of β -catenin results in relief of Tcf3-mediated repression at sites that are not reflected here by TOPGal activity. Precedence for a role for β -catenin in derepression of Tcf genes has been provided in lower eukaryotic systems (Cavallo et al., 1998).

In conclusion, the potent effects of loss of the repressor function of Tcf3 illustrate the requirement for the coalescence of transcriptional activators and repressors to properly define the temporal and spatial pattern of expression of AP axis inducing gene products. Although in vertebrates, the importance of the switch from repression to de-repression has often been overlooked in comparison with Wnt-mediated Lef/Tcf/ β -catenin activation, this study highlights the importance of Tcf3-mediated repression in shaping cell fate decisions for the establishment of the basic body plan. In the future, identification of target genes that require Tcf-mediated repression will accelerate our understanding of the role of Lef/Tcfs in governing cell fate determination.

We thank members of the Fuchs laboratory for helpful comments and critical reading of this manuscript, Nina Lampen for expert assistance with SEM experiments and Linda Degenstein for help with establishing the *Tcf3*^{-/-} lines. B.M. is supported by the American Cancer Society, and M.R. by a Schrodinger Fellowship. This work was funded by NIH grant AR31737.

References

- Ang, S. L. and Rossant, J. (1994). HNF-3 beta is essential for node and notochord formation in mouse development. *Cell* **78**, 561-574.
- Beddington, R. S. (1994). Induction of a second neural axis by the mouse node. *Development* **120**, 613-620.
- Bienz, M. and Clevers, H. (2003). Armadillo/beta-catenin signals in the nucleus—proof beyond a reasonable doubt? *Nat. Cell Biol.* **5**, 179-182.
- Brannon, M., Gomperts, M., Sumoy, L., Moon, R. T. and Kimelman, D. (1997). A beta-catenin/XTcf-3 complex binds to the siamois promoter to regulate dorsal axis specification in *Xenopus*. *Genes Dev.* **11**, 2359-2370.
- Brannon, M., Brown, J. D., Bates, R., Kimelman, D. and Moon, R. T. (1999). XctBP is a XTcf-3 co-repressor with roles throughout *Xenopus* development. *Development* **126**, 3159-3170.
- Brantjes, H., Roose, J., van de Wetering, M. and Clevers, H. (2001). All Tcf HMG box transcription factors interact with Groucho-related co-repressors. *Nucleic Acids Res.* **29**, 1410-1419.
- Cavallo, R. A., Cox, R. T., Moline, M. M., Roose, J., Polevoy, G. A., Clevers, H., Peifer, M. and Bejsovec, A. (1998). Drosophila Tcf and Groucho interact to repress Wingless signalling activity. *Nature* **395**, 604-608.
- Chan, S. K. and Struhl, G. (2002). Evidence that Armadillo transduces wingless by mediating nuclear export or cytosolic activation of Pangolin. *Cell* **111**, 265-280.
- Conlon, F. L., Lyons, K. M., Takaesu, N., Barth, K. S., Kispert, A., Herrmann, B. and Robertson, E. J. (1994). A primary requirement for nodal in the formation and maintenance of the primitive streak in the mouse. *Development* **120**, 1919-1928.
- DasGupta, R. and Fuchs, E. (1999). Multiple roles for activated LEF/TCF transcription complexes during hair follicle development and differentiation. *Development* **126**, 4557-4568.
- Dorsari, R. L., Itoh, M., Moon, R. T. and Chitnis, A. (2003). Two tcf3 genes cooperate to pattern the zebrafish brain. *Development* **130**, 1937-1947.
- Downs, K. M. and Davies, T. (1993). Staging of gastrulating mouse embryos by morphological landmarks in the dissecting microscope. *Development* **118**, 1255-1266.
- Galceran, J., Farinas, I., Depew, M. J., Clevers, H. and Grosschedl, R. (1999). Wnt3a^{-/-}-like phenotype and limb deficiency in Lef1^(-/-)Tcf1^(-/-) mice. *Genes Dev.* **13**, 709-717.
- Gat, U., DasGupta, R., Degenstein, L. and Fuchs, E. (1998). De Novo hair follicle morphogenesis and hair tumors in mice expressing a truncated beta-catenin in skin. *Cell* **95**, 605-614.
- Harland, R. and Gerhart, J. (1997). Formation and function of Spemann's organizer. *Annu. Rev. Cell Dev. Biol.* **13**, 611-667.
- Hensen, V. (1876). Uber ein neues Strukturverhaltis der quergestreiften muskelfaser. *Arb. Physiol. Inst. Kiel.* **1868**, 1-26.
- Hoodless, P. A., Pye, M., Chazaud, C., Labbe, E., Attisano, L., Rossant, J. and Wrana, J. L. (2001). FoxH1 (Fast) functions to specify the anterior primitive streak in the mouse. *Genes Dev.* **15**, 1257-1271.
- Houston, D. W., Kofron, M., Resnik, E., Langland, R., Destree, O., Wylie, C. and Heasman, J. (2002). Repression of organizer genes in dorsal and ventral *Xenopus* cells mediated by maternal XTcf3. *Development* **129**, 4015-4025.
- Huelsken, J., Vogel, R., Brinkmann, V., Erdmann, B., Birchmeier, C. and Birchmeier, W. (2000). Requirement for beta-catenin in anterior-posterior axis formation in mice. *J. Cell Biol.* **148**, 567-578.
- Ishikawa, T. O., Tamai, Y., Li, Q., Oshima, M. and Taketo, M. M. (2003). Requirement for tumor suppressor Apc in the morphogenesis of anterior and ventral mouse embryo. *Dev. Biol.* **253**, 230-246.
- Kim, C. H., Oda, T., Itoh, M., Jiang, D., Artinger, K. B., Chandrasekharappa, S. C., Driever, W. and Chitnis, A. B. (2000). Repressor activity of Headless/Tcf3 is essential for vertebrate head formation. *Nature* **407**, 913-916.
- Kinder, S. J., Tsang, T. E., Quinlan, G. A., Hadjantonakis, A. K., Nagy, A. and Tam, P. P. (1999). The orderly allocation of mesodermal cells to the extraembryonic structures and the anteroposterior axis during gastrulation of the mouse embryo. *Development* **126**, 4691-4701.
- Korinek, V., Barker, N., Morin, P. J., van Wichen, D., de Weger, R., Kinzler, K. W., Vogelstein, B. and Clevers, H. (1997). Constitutive transcriptional activation by a beta-catenin-Tcf complex in APC^{-/-} colon carcinoma. *Science* **275**, 1784-1787.
- Korinek, V., Barker, N., Moerer, P., van Donselaar, E., Huls, G., Peters, P. J. and Clevers, H. (1998a). Depletion of epithelial stem-cell compartments in the small intestine of mice lacking Tcf-4. *Nat. Genet.* **19**, 379-383.
- Korinek, V., Barker, N., Willert, K., Molenaar, M., Roose, J., Wagenaar, G., Markman, M., Lamers, W., Destree, O. and Clevers, H. (1998b). Two members of the Tcf family implicated in Wnt/beta-catenin signaling during embryogenesis in the mouse. *Mol. Cell Biol.* **18**, 1248-1256.
- Lawson, K. A., Meneses, J. J. and Pedersen, R. A. (1991). Clonal analysis of epiblast fate during germ layer formation in the mouse embryo. *Development* **113**, 891-911.
- Liu, P., Wakamiya, M., Shea, M. J., Albrecht, U., Behringer, R. R. and

- Bradley, A. (1999). Requirement for Wnt3 in vertebrate axis formation. *Nat. Genet.* **22**, 361-365.
- Lu, C. C., Brennan, J. and Robertson, E. J. (2001). From fertilization to gastrulation: axis formation in the mouse embryo. *Curr. Opin. Genet. Dev.* **11**, 384-392.
- Maretto, S., Cordenonsi, M., Dupont, S., Braghetta, P., Broccoli, V., Hassan, A. B., Volpin, D., Bressan, G. M. and Piccolo, S. (2003). Mapping Wnt/beta-catenin signaling during mouse development and in colorectal tumors. *Proc. Natl. Acad. Sci. USA* **100**, 3299-3304.
- Meno, C., Gritsman, K., Ohishi, S., Ohfujii, Y., Heckscher, E., Mochida, K., Shimono, A., Kondoh, H., Talbot, W. S., Robertson, E. J. et al. (1999). Mouse Lefty2 and zebrafish antivin are feedback inhibitors of nodal signaling during vertebrate gastrulation. *Mol. Cell* **4**, 287-298.
- Merrill, B. J., Gat, U., DasGupta, R. and Fuchs, E. (2001). Tcf3 and Lef1 regulate lineage differentiation of multipotent stem cells in skin. *Genes Dev.* **15**, 1688-1705.
- Morin, P. J., Sparks, A. B., Korinek, V., Barker, N., Clevers, H., Vogelstein, B. and Kinzler, K. W. (1997). Activation of beta-catenin-Tcf signaling in colon cancer by mutations in beta-catenin or APC. *Science* **275**, 1787-1790.
- Mukhopadhyay, M., Shtrom, S., Rodriguez-Esteban, C., Chen, L., Tsukui, T., Gomer, L., Dorward, D. W., Glinka, A., Grinberg, A., Huang, S. P. et al. (2001). Dickkopf1 is required for embryonic head induction and limb morphogenesis in the mouse. *Dev. Cell* **1**, 423-434.
- Perea-Gomez, A., Vella, F. D., Shawlot, W., Oulad-Abdelghani, M., Chazaud, C., Meno, C., Pfister, V., Chen, L., Robertson, E., Hamada, H. et al. (2002). Nodal antagonists in the anterior visceral endoderm prevent the formation of multiple primitive streaks. *Dev. Cell* **3**, 745-756.
- Popperl, H., Schmidt, C., Wilson, V., Hume, C. R., Dodd, J., Krumlauf, R. and Beddington, R. S. (1997). Misexpression of Cwnt8C in the mouse induces an ectopic embryonic axis and causes a truncation of the anterior neuroectoderm. *Development* **124**, 2997-3005.
- Reya, T., Duncan, A. W., Ailles, L., Domen, J., Scherer, D. C., Willert, K., Hintz, L., Nusse, R. and Weissman, I. L. (2003). A role for Wnt signalling in self-renewal of haematopoietic stem cells. *Nature* **423**, 409-414.
- Roose, J., Molenaar, M., Peterson, J., Hurenkamp, J., Brantjes, H., Moerer, P., van de Wetering, M., Destree, O. and Clevers, H. (1998). The Xenopus Wnt effector XTcf-3 interacts with Groucho-related transcriptional repressors. *Nature* **395**, 608-612.
- Sasaki, H. and Hogan, B. L. (1996). Enhancer analysis of the mouse HNF-3 beta gene: regulatory elements for node/notochord and floor plate are independent and consist of multiple sub-elements. *Genes Cells* **1**, 59-72.
- Skromne, I. and Stern, C. D. (2001). Interactions between Wnt and Vg1 signalling pathways initiate primitive streak formation in the chick embryo. *Development* **128**, 2915-2927.
- Sulik, K., Dehart, D. B., Iangaki, T., Carson, J. L., Vrablic, T., Gesteland, K. and Schoenwolf, G. C. (1994). Morphogenesis of the murine node and notochordal plate. *Dev. Dyn.* **201**, 260-278.
- Travis, A., Amsterdam, A., Belanger, C. and Grosschedl, R. (1991). LEF-1, a gene encoding a lymphoid-specific protein with an HMG domain, regulates T-cell receptor alpha enhancer function. *Genes Dev.* **5**, 880-894.
- van Genderen, C., Okamura, R. M., Farinas, I., Quo, R. G., Parslow, T. G., Bruhn, L. and Grosschedl, R. (1994). Development of several organs that require inductive epithelial-mesenchymal interactions is impaired in LEF-1-deficient mice. *Genes Dev.* **8**, 2691-2703.
- van de Wetering, M., Oosterwegel, M., Dooijes, D. and Clevers, H. (1991). Identification and cloning of TCF-1, a T lymphocyte-specific transcription factor containing a sequence-specific HMG box. *EMBO J.* **10**, 123-132.
- van de Wetering, M., Sancho, E., Verweij, C., de Lau, W., Oving, I., Hurlstone, A., van der Horn, K., Battle, E., Coudreuse, D., Haramis, A. P. et al. (2002). The beta-catenin/TCF-4 complex imposes a crypt progenitor phenotype on colorectal cancer cells. *Cell* **111**, 241-250.
- Verbeek, S., Izon, D., Hofhuis, F., Robanus-Maandag, E., te Riele, H., van de Wetering, M., Oosterwegel, M., Wilson, A., MacDonald, H. R. and Clevers, H. (1995). An HMG-box-containing T-cell factor required for thymocyte differentiation. *Nature* **374**, 70-74.
- Vincent, S. D., Dunn, N. R., Hayashi, S., Norris, D. P. and Robertson, E. J. (2003). Cell fate decisions within the mouse organizer are governed by graded Nodal signals. *Genes Dev.* **17**, 1646-1662.
- Weinstein, D. C., Ruiz i Altaba, A., Chen, W. S., Hoodless, P., Prezioso, V. R., Jessell, T. M. and Darnell, J. E., Jr (1994). The winged-helix transcription factor HNF-3 beta is required for notochord development in the mouse embryo. *Cell* **78**, 575-588.
- Wilkinson, D. G. and Nieto, M. A. (1993). Detection of messenger RNA by in situ hybridization to tissue sections and whole mounts. *Methods Enzymol.* **225**, 361-373.
- Wilkinson, M. F. and Shyu, A. B. (2002). RNA surveillance by nuclear scanning? *Nat. Cell Biol.* **4**, E144-E147.
- Yamamoto, M., Meno, C., Sakai, Y., Shiratori, H., Mochida, K., Ikawa, Y., Saijoh, Y. and Hamada, H. (2001). The transcription factor FoxH1 (FAST) mediates Nodal signaling during anterior-posterior patterning and node formation in the mouse. *Genes Dev.* **15**, 1242-1256.
- Zeng, L., Fagotto, F., Zhang, T., Hsu, W., Vasicek, T. J., Perry, W. L., 3rd, Lee, J. J., Tilghman, S. M., Gumbiner, B. M. and Costantini, F. (1997). The mouse Fused locus encodes Axin, an inhibitor of the Wnt signaling pathway that regulates embryonic axis formation. *Cell* **90**, 181-192.
- Zhou, P., Byrne, C., Jacobs, J. and Fuchs, E. (1995). Lymphoid enhancer factor 1 directs hair follicle patterning and epithelial cell fate. *Genes Dev.* **9**, 700-713.